Single-cell imaging of *Pseudomonas* reveals dynamic polar accumulation of the extracellular iron-scavenger pyoverdin

Clara Moreno-Fenoll[1,2,*], Maxime Ardré[2], and Paul B. Rainey[1,2]

[1]Laboratory of Biophysics and Evolution, CBI, ESPCI Paris, Université PSL, CNRS, 75005 Paris, France

[2]Department of Microbial Population Biology, Max Planck Institute for Evolutionary Biology, Plön, Germany

[*]Corresponding author: cmorenofenoll@evolbio.mpg.de

Abstract

Pyoverdin is a water-soluble metal-chelator synthesized by members of the genus *Pseudomonas* and used for the acquisition of insoluble ferric iron. Although freely diffusible in aqueous environments, preferential dissemination of pyoverdin among adjacent cells, fine-tuning of intracellular siderophore concentrations, and fitness advantages to pyoverdin-producing versus nonproducing cells, indicate control of location and release. Here, using time-lapse fluorescence microscopy to track single cells in growing microcolonies of *Pseudomonas fluorescens* SBW25, we show accumulation of pyoverdin at cell poles. Accumulation is induced by arrest of cell division, is achieved by cross-feeding in pyoverdin-nonproducing mutants, is independent of cell shape, and is reversible. Furthermore, it occurs in multi-species communities. Analysis of the performance of pyoverdin-producing and nonproducing cells under conditions promoting polar localization shows an advantage to accumulation on resumption of growth after stress. While the genetic basis of polarization remains unclear, evaluation of deletion mutants of pyoverdin transporters (*opmQ*, *fpvA*) establishes non-involvement of these candidate loci. Examination of pyoverdin polar accumulation in a model community and in a range of laboratory and natural species of *Pseudomonas*, including *P. aeruginosa* PAO1 and *P. putida* KT2440, confirms that the phenotype is characteristic of *Pseudomonas*.

Significance

Bacteria secrete extracellular products that enable nutrients to be obtained from the environment. A secreted product of relevance for medicine, agriculture and biotechnology is the iron-chelating

siderophore, pyoverdin, which is produced by members of the genus *Pseudomonas*. By analyzing the behavior of single cells we show that on cessation of cell division, pyoverdin localizes to cell poles, but is then released to the environment prior to resumption of cell growth. Of particular significance is the ecological relevance of this behavior: cells that accumulate the siderophore resume growth with minimal delay. Our study reveals a hitherto unrecognized dimension to the biology of *Pseudomonas* that may prove central to understanding the broader ecological and physiological relevance of pyoverdin.

Introduction

Extracellular secreted products perform important functions in microbial communities. They provide structure and protection [1], enable coordinated action [2] [3] and also allow acquisition of recalcitrant nutrients, such as polymers that are too large to be internalized [4], or are otherwise unavailable. An example of the latter is pyoverdin.

Pyoverdin is a naturally fluorescent iron-scavenging chelator (sideropohore) produced by members of the genus *Pseudomonas* [5]. Iron is an essential micronutrient that exists in an insoluble state (ferric) in aerobic environments [6]. In response to intracellular iron scarcity, pyoverdin biosynthesis begins in the cytoplasm via nonribosomal peptide synthesis and undergoes maturation in the periplasm [7]. After secretion, it binds Fe^{3+} with high affinity (Ka $= 10^{32}$ M^{-1} for PVDI produced by *P. aeruginosa* PAO1 [8]). Once bound to ferric iron the ferripyoverdin complex loses its fluorescent properties, but is recognized by a specific receptor (FpvA) and imported back into the periplasm, where iron is extracted. The apo-pyoverdin molecule is then recycled and can undergo further cycles of export and import [9].

Because pyoverdin is a soluble extracellular product, it has been widely assumed to be equally available to all members of a community [10–12]. However, recent work shows that its distribution is subject to cell-level control. In one study pyoverdin producers retained an environment-dependent fitness advantage in conditions where invasion by nonproducers was expected. In light of these experimental results, the possibility of personalization was raised [13]. Other studies have further supported this notion. For example, in growing microcolonies, pyoverdin diffuses primarily between adjacent cells, reducing loss into the environment [14]. Furthermore, *Pseudomonas aeruginosa* cells tune periplasmic concentrations of pyoverdin in order to protect against oxidative stress [15].

Here we use time-lapse fluorescence microscopy to study the relationship between *P. fluorescens* SBW25 cells and pyoverdin. Recognizing the importance of spatial structure and contributions therefrom to μm-scale features of microbial assemblages [16–19], cells were grown on thin layers of agarose set on top of microscope slides. In actively dividing cells, naturally fluorescent apo-pyoverdin is evenly distributed in the periplasm, however, on cessation of growth we observed

pyoverdin to localize to cell poles. This surprising discovery motivated quantitative analysis, revealing the process of localization to be dynamic, reversible, and ecologically relevant.

Results

P. fluorescens SBW25 (herafter SBW25) is a model bacterium [20] known to produce pyoverdin [21] and other secreted products [22, 23]. In a previous study of pyoverdin, Zhang & Rainey [13] provided evidence of pyoverdin personalization that was inferred following contrasting outcomes of fitness assays in different conditions. We reproduced these assays, but rather than examining frequencies of producers and nonproducers by plating, aliquotes were observed by fluorescence microscopy. In casamino acids medium (CAA), the medium where an unexpected advantage for pyoverdin producers had been described, cells exhibited fluorescent foci (Fig. 1 A). This initial observation motivated further analysis.

To accurately characterize subcellular patterns of pyoverdin, time-lapse fluorescence images of ancestral SBW25 were obtained in defined succinate minimal medium (SMM), where succinate acts both as carbon source and weak iron chelator. During exponential phase and early stationary phase, SBW25 cells present the phenotype typical of fluorescent *Pseudomonas* with pyoverdin being homogeneously distributed in the periplasm. However, in late stationary phase a different phenotype emerges that involves accumulation of pyoverdin at the cell pole. Polarization of pyoverdin is evident by qualitative observation (Fig. 1 B) and was verified after image analysis and segmentation by superposing fluorescence profiles at different time points. (Fig. 1 C).

By examining cell division throughout the time-lapse series it is possible to connect time to population growth. Mean age of cells in the population highlights these different physiological states. The corresponding frequency of polarized cells (Fig. 2 A) was tracked by classifying segmented cells automatically as "polarized" and "homogeneous" using a machine learning algorithm (Supplementary Materials and Methods). After inoculating the microscope slide, cells undergo a period of acclimation to the medium without division. We observed no polarization events during this lag phase. As division begins, age of cells in microcolonies decreases until it reaches a minimum that marks exponential phase. Bacteria continued to be non-polarized. Note that the small frequency of cells identified as "polarized" in the plot falls within the range of classification errors. Finally, the population enters stationary phase and cells continue ageing without division. Polarization increased within the first few hours, encompassing a majority cells within the population at 18h (Fig. S1).

While the time-averaged state of microcolonies exposes population-level dynamics of polarization – namely, that polarization happens in stationary phase – it obscures the behavior of individual cells. To specifically analyze single cells, cells were grouped according to their division status over three generations: F0 for initial inoculum (cells where birth could not be identified but division was observed), F1 for cells in exponential phase (born from the division of F0 cells and

underwent division later) and F2 for the daughter cells of F1 that entered stationary phase and remained constant for the final hours of the experiment. Growth measurements from F1 cells, and pyoverdin accumulation measurements from F2, corroborate, that despite some variability in the onset of polarization, polarization appears to be strictly incompatible with active cell division. Cells either elongate or accumulate fluorescence (pyoverdin) at the cell pole. This result holds for both the old and new pole (Fig. 2 B). Curiously, the siderophore accumulates preferentially at the new pole, but not exclusively, and sometimes distinct foci are present at both (Fig. S2.))

Stationary phase marks cessation of cell division due to nutrient depletion. To investigate the effect of other environmental stresses that interfere with cell division on polarization, bacteria were treated with either 2,2'-dipyridil (DP, an iron chelator) or tetracycline at concentrations where no division was observed during 8 h (Fig. S3 A) . Both stresses induced polarization (Fig 2 C). Since the treatments included chemicals both related and unrelated to pyoverdin regulation, a iron-chelator and antibiotic, respectively, arrest of cell division is likely the trigger for the polar-accumulation phenotype, rather than a specific environmental cue, such as nutrient depletion.

Precisely because polarization appears when cells are starved and/or stressed, processes associated with cell death, such as cell wall damage, are potential elicitors. Based on ability to reliably induce polarization by adding an iron chelator (Fig 2 C) a protocol was developed to assess the viability of cells with polarized pyoverdin. This involved transfer of bacteria pre-treated with DP to a fresh agarose pad. Time-lapse imaging of these cells revealed that polarization is reversible and precedes exit from lag phase (Fig 2 D). Polarized cells consistently re-established a homogeneous pyoverdin distribution within the first few hours after inoculation, with elongation and division resuming at a later time point (Fig. S3 B). Note that both the initial frequency of polarized cells and the time to depolarization were counted from from the start of image acquisition. During the previous experimental manipulation, some individuals might have altered their polarization status. Despite this, the trend is clear, with depolarization occurring before resumption of growth. Polarization is thus not a consequence of cell death but rather a reversible, dynamic process tied to arrest of cell division.

To explore population-level consequences of pyoverdin accumulation, growth delay of cells was measured in a range of environments where pyoverdin has physiological relevance. SBW25, or the pyoverdin nonproducing mutant *pvdS229*(D77N) [13] (termed Pvd$^-$ here), were pre-grown either in iron-restrictive or permissive SMM and then transferred to fresh SMM medium. Comparing conditions in which pyoverdin is polarized and not polarized, and cells that can and cannot accumulate pyoverdin, stands as a test for functional implications arising from polarization. To ensure that the observed effects are related to iron deprivation and ensuing effects of pyoverdin on physiology, all tested conditions also received a supplement of excess iron. In non-restrictive conditions, without chelator supplementation, pyoverdin did not introduce a substantial difference: SBW25 and Pvd$^-$ showed similar lag times before resuming division in fresh medium. Iron supplementation did not modify lag times (Fig 3 A, left). However, exposure to iron-deprived conditions led to a considerable delaye in the time to the first cell division for cells that had no accumulated pyoverdin. SBW25 cells

with polarized pyoverdin also showed longer lag phases after iron deprivation, but to a much lesser extent. In these conditions iron supplementation had a significant impact, again reducing the lag phase of the non-producer mutant to values similar to the ancestral producer (Fig. 3 A, right). This suggests that pyoverdin stockpiled at the cell poles during conditions where it is presumably not used (pyoverdin accumulates when cells are not dividing), enables faster recovery when the environment is again amenable to growth.

Dissociation of pyoverdin from the cell pole does not necessarily imply that it has been secreted. Intracellular iron can cause toxic oxygen reactive species, and the siderophore is known to protect cells from oxidative damage while remaining in the periplasm [15]. To distinguish this from an effect derived from pyoverdin in the external medium, we separately deprived both SBW25 and nonproducer cells of iron, and then co-inoculated both strains on the same fresh agarose pad. In this setting, changes in behavior of the nonproducer can be reasonably attributed to pyoverdin released by the producer. Upon co-inoculation, mutants displayed reduced lag times comparable to ancestral SBW25 (Fig. 3 B). Pyoverdin is thus secreted by the producer after depolarization and used by both strains to acquire essential iron from the environment. Furthermore, the amount of pyoverdin accumulated during starvation seems to be enough to support at least twice as many cells, as the lag time of SBW25 producer cells was not affected by the presence of nonproducers. This result is in line with other work, where populations of siderophore-producing *Pseudomonas* were shown to grow in the presence of numerous nonproducing mutants without causing a significant reduction in yield [24].

Pyoverdin polarization seems to be tied to particular physiological states. Just how polarization is integrated within the biology of cells requires mechanistic molecular knowledge. We envisioned different scenarios that might lead to transport of pyoverdin to cell poles and subsequent accumulation. One possibility is that pyoverdin is passively accumulated at the cell pole as a consequence of the rod shape of *Pseudomonas* cells. Alternatively, localization could be driven by specific biomolecular features of the cell pole, for example, transport via proteins that recognize signals of polar identity. Either of these processes could in turn be unique to pyoverdin, or general phenomena affecting the contents of the periplasm of SBW25. To investigate these possiblities we examined mutants with specific gene deletions, both in the pyoverdin pathway and in other cellular processes that could be feasibly involved in polarization.

First, we verified that the accumulated pyoverdin is mature and functioning, as opposed to being an aberrant molecular form with defective periplasmic maturation [25]. Cross-feeding experiments (Fig. 3 B) demonstrate that nonproducers can use pyoverdin secreted by SBW25 producer cells where pyoverdin was previously polarized. However, this does not eliminate the possibility that polarized pyoverdin is structurally defective; for example, polarization and growth recovery could be caused by different pyoverdin molecules, with the former being non-functional. To test this, SBW25 producer and nonproducer types (the latter with an mCherry fluorescent marker) were co-cultured. After overnight growth (17 h in the conditions previously described, Fig. 1) colonies of the nonproducer had polarized pyoverdin (Fig. 4.1). This indicates that polarized

pyoverdin is functional, since any siderophore internalized by Pvd$^-$ necessarily comes from the external medium after export by SBW25. Polarization thus involves pyoverdin that is actively used among cells of the population.

Next, we considered trafficking of pyoverdin across the periplasm. An imbalance could lead to an excess of molecules aggregating at the exporter or the receptor, which in turn could result in polarization [26, 27]. After deleting the gene encoding the efflux pump OpmQ, intracellular levels of pyoverdin increased (Fig. S4 A), but secretion was not completely abolished. This is not surprising as it is known that additional pyoverdin transporters exist, although their identity is largely unknown [28]. This Δ*opmQ* mutant, however, displayed polarization similar to SBW25, thus eliminating OpmQ as a candidate for the mechanism (Fig. 4.2).

Unravelling a role for the ferripyoverdin receptor FpvA is more complicated, because synthesis, via a positive feedback loop, is determined by the interaction between ferripyoverdin and the FpvA receptor. As a consequence, Δ*fpvA* mutants produce only basal levels of the siderophore [7] (Fig. S4 B). Nevertheless, a small fraction of cells manufactured pyoverdin at higher levels - possibly due to noise in the gene regulatory circuits. In these cells fluorescence accumulation at the pole was observed (Fig. 4.3). FpvA is therefore not directly responsible for polarization. Additional possibilities for localization are conceivably connected to extracellular polymer synthesis and cell morphology. SBW25 secretes cellulose which can act as a glue for the construction of bacterial mats at the air-liquid interface [23]. This sticky polymer could trap the iron scavenger in an extracellular mesh attached to the cell. However, the cellulose nonproducer Δ*wsp*Δ*aws*Δ*mws* [29] polarizes pyoverdin in a manner comparable to ancestral SBW25 (Fig. 4.4). Finally, the rod-cell-shape that is characteristic of *Pseudomonas* was considered as a possible contributory factor. To test this we looked for pyoverdin accumulation in a spherical Δ*mreB* mutant. Despite the spherical shape, this strain displayed fluorescence foci after extended culture (Fig. 4.5). The mechanistic details of pyoverdin polarization remain to be discovered, but mutants analyzed here constrain the range of possibilities. The most readily available explanations that involve imbalances in pyoverdin trafficking are largely eliminated, and the behavior of Δ*mreB* indicates that siderophore transport to the poles is not an incidental consequence of cell shape.

We further tested pyoverdin polarization in conditions closer to the natural milieu of SBW25, where species interdependencies are common and resources invariably limiting. To implement a minimal bacterial community, SBW25 was co-cultured with a cellulose-degrading *Bacillus* isolated from a compost heap [30]. Because SBW25 is unable to degrade this polymer, it must rely on the *Bacillus* species to obtain carbon for growth. These two strains were grown together in minimal medium with cellulose paper as the sole carbon source and periodically imaged to assess polarization status. Pyoverdin was readily observed to be polarized (Fig 5 A). Pyoverdin accumulation at the cell pole is thus likely to be part of the natural phenotypic repertoire of SBW25, and given that conditions such as those experienced here are likely typical, polarization of pyoverdin might be the normal state.

Since pyoverdins are produced by many species of the genus *Pseudomonas*, investigating subcellular distribution in related strains stands to provide an evolutionary context for polar accumulation. We selected 11 strains belonging to the genus *Pseudomonas*, comprising both common laboratory strains (such as *P. aeruginosa* PAO1, in which pyoverdin is usually studied) and natural isolates from different European locations. The ability of these strains to polarize pyoverdin was classified qualitatively, that is, presence or absence of polarized cells (Fig 5 B.) All tested strains localized pyoverdin at the cell poles in conditions similar to those described here for SBW25. Interestingly, different strains polarized pyoverdin with treatments of varying stringency. In some cases extended culture in SMM was enough to observe the phenotype (eg. *P. putida* KT2440). In others, amendment with an iron chelator was necessary to observe the effect (eg. *P. aureofaciens* U149), at the same dosage that induced polarization in SBW25, and in the specific case of *P. aeruginosa* PAO1, very high doses of DP were required. This range of responses could reflect the secretion of secondary siderophores by some strains [32] or differences in the regulation of pyoverdin production [12], and suggest that polarization is an ecologically relevant trait that varies depending on the evolutionary history of the lineage.

Discussion

Previous work showing that the population-level distribution of pyoverdin changes depending on nutrient status [13], contact with neighboring cells [14], or environmental stress [15] motivated our investigation. With focus on *P. fluorescens* SBW25, and using time-resolved microscopy, we have shown that pyoverdin transiently accumulates at cell poles; and that localization is a reversible process associated with arrest of cell division and affected by factors such as entry into stationary phase, deprivation of specific nutrients, and antibiotic treatment (Fig 2). Particularly significant is demonstration that accumulation of pyoverdin has ecological relevance.

Dynamic localization of proteins at bacterial cell poles is not unusual: various cellular structures are localized to either new or old poles [33]. In some instances, localization is determined via specific protein interactions, while in others, mechanisms, involving, for example, nuclear occlusions at the cytoplasm, are responsible [34]. In *P. aeruginosa* complexes termed "siderosomes" form by association of the enzyme L-ornithine N5-oxygenase (encoded by *pvdA*) with the cytoplasmic membrane, causing pyoverdin synthesis to be localized to old cell poles [35, 36].

The possibility that pyoverdin synthesis might be connected to pyoverdin accumulation was considered plausible, although unlike accumulation observed in SBW25, siderosomes are active during exponential growth and localized primarily to old cell poles. Evidence that indicates synthesis and accumulation are determined by distinct processes stems from analysis of SBW25 cells devoid of functional *pvdS* (Pvd^-, Fig. 4) – and thus devoid of all enzymes necessary for synthesis of pyoverdin (including *pvdA*). When co-cultured with SBW25 pyoverdin-producing cells, *pvdS* mutant cells accumulated pyoverdin from the external environment at the cell poles. Transcription of pyoverdin

biosynthetic genes is thus not required for polar accumulation of pyoverdin.

Recognition that pyoverdin accumulation is unconnected to synthesis caused attention to shift to involvement of pyoverdin uptake and recycling systems. To this end, genes encoding the primary outer membrane receptor for the ferri-pyoverdin complex, FpvA, and primary component of the pyoverdin recycling (export) system, OmpQ, were deleted. Both Δ*fpvA* and Δ*opmQ* were able to accumulate and localize pyoverdin (Fig. 4). While thus far we have failed to identify any genetic basis for accumulation, ability to rule out primary and obvious candidates narrows the scope for future investigations.

While pyoverdin was found most often accumulated at the new pole, it was also observed at the old pole, and on occasion it was found at both poles. Lack of location specificity hints at a connection to more general biophysical aspects of cell biology. Interestingly, a recent study of *E. coli* under starvation conditions showed polar accumulation of fluorescent markers, including mCherry [37]. Accumulation was connected to shrinkage of the cytoplasm, with shrinkage creating additional space in the polar region of the periplasm.

Certain of the dynamics observed by Shi et al (2021) [37] are consistent with our observations, however, some observations are difficult to reconcile with experimental details and the known biology of pyoverdin. For example, polarization of mCherry occurred in the periplasm of *E. coli* soon after starvation, but these cells maintained high ATP levels typical of exponentially growing cells. There is no reason to assume that such metabolically active cells would be compromised in ability to import or export pyoverdin, and therefore it is difficult to conceive of reasons why SBW25 would begin to accumulate pyoverdin if metabolic activity was not compromised. Further, pyoverdin, a small diffusible molecule, is unlikely to behave as observed for an engineered periplasm-targeted mCherry reporter. In *E.coli* cytoplasmic contraction occurs upon starvation and was not affected by antibiotic treatment. In contrast, in SBW25, localized accumulation of pyoverdin occurred under starvation conditions, but also on cessation of growth caused by addition of tetracycline to cells present in an otherwise resource-permissive environment (Fig. 2 C). Also of relevance are our investigations of the distribution of pyoverdin in spherical Δ*mreB* cells. Despite absence of poles, pyoverdin accumulated in discrete regions on starvation (Fig. 4). It would be interesting to investigate localization of mCherry in morphology mutants of *E.coli*.

Irrespective of the mechanism, whether it be connected to cytoplasmic shrinkage, some other physical aspect of cell biology, determined by a specific genetic pathway, or a combination of physical and genetic factors, our results demonstrate that localization of pyoverdin has ecological significance. Data in Fig. 3 A show that cells with localized pyoverdin resume growth more rapidly than cells that have not accumulated reserves of pyoverdin. This time-to-first cell division advantage was not evident when growth-arrested cells were transferred to iron-replete conditions. This demonstrates that liberation of the stock of pyoverdin accumulated during growth cessation has fitness consequences, presumably through provision of available iron to growing cells, as Fig. 3 B indicates.

The seemingly adaptive nature of pyoverdin accumulation under stress is reminiscent of – and perhaps even connected to – the capacity of SBW25 to enter a semiquiescent capsulated state upon starvation. Counter to received wisdom, during starvation, SBW25 cells produce an excess of ribosomes that allow rapid exit from stationary phase once growth-permissive conditions are encountered. Cells unable to provision ribosomes are quickly out-competed by those that do [38]. It is possible that localization of pyoverdin, followed by fast release under growth permissive conditions, has evolved as a strategy precisely because it maximizes competitive performance upon resumption of growth. The decision to enter stationary phase is just as significant as the means of exiting. Rapid resumption of growth is likely to deliver significant fitness benefits in environments punctuated by periods of nutrient abundance and scarcity.

There has been a tendency to observe diffusible products through the lens of social evolution theory, where products are viewed as public goods, and producers and nonproducers considered players in a game of prisoner's dilemma. Accordingly, populations of producers, when rare, should not invade populations of nonproducers. This expectation arises from a presumed cost to production, combined with the assumption that the extracellular product is equally available to both producers and nonproducers. However, a number of studies have shown that this simple expectation does not always hold, leading to the suggestion that producers might gain preferential access to the secreted product [12, 13, 39, 40].

Investigations at the level of individual cells have proved essential for linking behavior of cells to the dynamics of populations [17, 18]. For example, Gore et al (2009) [39] showed that the cellular location of invertase responsible for degradation of sucrose in *Saccharomyces cerevisiae* creates diffusion gradients of degradation products that deliver benefit to producing cells, despite cost to producers of synthesizing the enzyme [39]. Similarly, the siderophore enterochelin (a catecholate secreted by *E. coli* and other *Enterobacteriaceae*) can remain associated with the outer membrane under conditions of low cell density, delivering preferential benefit to enterochelin-producing cells [40]. Our findings show clear evidence that pyoverdin can be localized, and while localization also occurs in nonproducing mutants (via uptake from producer cells) – and can deliver fitness benefits to nonproducers – producers consistently show a faster time to the first cell division (Fig. 3) compared to nonproducing types. This is in agreement with data showing that producers can gain preferentially from the product they synthesize [13]. It is likely that behaviors such as those observed here are important contributors to population – and even community – dynamics in natural environments.

The eco-physiology of pyoverdin is complex and poorly understood. Advances in understanding are key to making biological, ecological and evolutionary sense of behaviors such as those described here [12, 41]. Complexity arises at the physiological level from the interplay between the redox status of iron (that affects bio-availability), and cellular demands that are balanced against potentially lethal toxic effects. For example, in aerobic environments, where bio-availability of iron is low and cellular demand high, cells risk harm from hydroxyl radicals liberated via the Fenton reaction. One role of pyoverdin is as protectant against intracellular oxidative stress [15]. But pyoverdin has roles beyond iron-specific chemistry: pyoverdin chelates other metals, including magnesium, zinc

and gallium, with roles in homeostasis and detoxification of these and other metals [28]. Challenges arise from the need to understand the ecological relevance of numerous diverse forms of pyoverdin [32], the plethora of ferri-pyoverdin receptors [42, 43], and the various roles of pyoverdin in shaping interactions with eukaryotic hosts [44–46].

Complexity further escalates once pyoverdin is placed in context of microbial communities, where roles for pyoverdin are evident [47–52], and where community function affects physico-chemical factors such as pH, viscosity, moisture, and resources (type and abundance), all of which are subject to frequent change [53, 54]. Although we have not delved into these complexities, the fact that pyoverdin is accumulated and localized under growth limiting conditions in a diverse range of *Pseudomonas*, combined with evidence of the same behavior in SBW25 cells grown for weeks under nutrient restrictive conditions with reliance on cellulose degrading *Bacillus* (Fig. 5), suggests that polarization has relevance to conditions beyond those experienced by cells in standard, nutritionally-rich, exponential-phase, laboratory culture.

Materials and methods

Strains, culture media, and reagents. Ancestral *Pseudomonas fluorescens* SBW25 originally isolated on beet roots at the University of Oxford farm (Wytham, Oxford, U.K.) [20] and a collection of relevant mutants were used: the pyoverdin nonproducer *pvdsG229A*(D77N) named Pvd$^-$ in the main text (construction described in [13]), the corresponding strain with mCherry fluorescence tagging under IPTG induction, Δ*mreB*, PBR716 (Δ*wsp*Δ*aws*Δ*mws*, described in [29]). Pyoverdin import and export defective mutants Δ*PFLU3979* (OpmQ) and Δ*PFLU2545* (FpvA) were created by two-step allelic exchange [55]. A neutrally marked SBW25 strain [56] was used to replicate the fitness assays from [13]. *Escherichia coli* DH5α λ_{pir} and pRK2013 were used for cloning. *Bacillus* 002.IH from Steven Quistad's compost heap collection [30] was used for the community experiment. For the phylogenetic comparison, an assortment of species of the genus *Pseudomonas* were selected from the lab collection. Most experiments were performed in succinate minimal medium (SMM, described in [14]). Overnight cultures were done in Luria-Bertani (LB) broth. Replication of fitness assays was performed in CAA and KB media as described in the original work [13]. Community experiment was done in M9 minimal medium with cellulose as the only carbon source (Whatman). Where indicated media was supplemented with 2,2'-dipyridil (Sigma), tetracycline (Duchefa, France), $Fe_2[SO_4]_3$(III) (Sigma), IPTG (Melford). For strain construction tetracycline, nitrofurantoin (Sigma), X-gal (Melford), D-cycloserine (Duchefa) were used.

Agarose pad.To prepare the agarose pad, 220 μL of agarose (Melford) dissolved in SMM (2% w/v) were poured onto a microscope slide fitted with a sticky frame (Gene Frame, Fisher Scientific), pressed with a clean slide and allowed to dry for $\sim$ 2 min. A small $\sim$ 3 mm section of the pad and frame was cut across the slide to provide air for the growing cells. 1.5 μL of washed culture was inoculated on the agarose pad and sealed with a coverslip.

Microscopy. Inoculated agarose pads were monitored by taking snapshots every 30 min for a typical total time of 18h using the microscope Axio Observer.Z1 (Zeiss, Germany). Cells were imaged under phase contrast (exposure: 30 ms) and fluorescence corresponding to Pvd using the fluorescence Source X-Cite 120 LED and the following filters: 390/40 BrightLine HC, Beamsplitter T 425 LPXR, 475/50 BrightLine HC (exposure: 30 ms, 12 % intensity). Images were taken with 63x and optovar 1.6x magnification.

Image analysis. Image processing was performed using the image analysis software Image J. Segmentation and analysis was performed using the package for Matlab SuperSegger from the Wiggins Lab [57]. Further analysis and data visualization was carried out with the programming software R. After segmentation cells were sorted by polarization status using a classificator obtained with the Statistics and Machine Learning Toolbox for Matlab (More information in Supplementary Methods).

Community experiment. SBW25 and *Bacillus* 002.IH (from [30]) were grown on 20 ml M9 minimal medium and cellulose as the only carbon source (1 cm x 1 cm cellulose paper). After overnight growth cultures were washed and co-inoculated into 20 ml of M9 medium with cellulose paper in a 60 ml vial. These vials were incubated at room temperature with unscrewed caps to allow air exchange, and periodically sampled for imaging.

Phylogenetic comparison. A collection of laboratory and natural strains belonging to the genus *Pseudomonas* were subjected to a binary qualitative polarization test, i.e. the test was considered positive if polarized cells were observed under fluorescence microscopy in conditions similar to SBW25 but no dynamics were assessed. Commonly used laboratory strains *P. aeruginosa* PAO1 and *P. putida* KT2440 were tested. Natural isolates belong to collections from two different locations. Paris, France [30]: T24 V1a, T24 V9b, T24 H1b, T24H9b; all classified as *P. putida*. Oxford, UK [31]: *P. marginalis* U106, *P. putida* U177, *P.aureofaciens* U149, U180, and U181.

Author contributions

PBR, CMF and MA designed research. CMF performed research. CMF and MA analyzed data. PBR, CMF and MA wrote the paper.

Conflicts of interest

The authors declare no competing interests.

Acknowledgements

We thank Dave Rogers for assistance with construction of mutants. We thank Steven D. Quistad and Xue-Xian Zhang for natural strain collections. PBR acknowledges generous core support from the Max Planck Society.

References

1. Flemming, H.-C. *et al.* Biofilms: an emergent form of bacterial life. *Nature Reviews Microbiology* **14,** 563–575 (2016).
2. Newman, J. W., Floyd, R. V. & Fothergill, J. L. The contribution of Pseudomonas aeruginosa virulence factors and host factors in the establishment of urinary tract infections. *FEMS Microbiology Letters* **364** (2017).
3. Diard, M. *et al.* Stabilization of cooperative virulence by the expression of an avirulent phenotype. *Nature* **494,** 353–356 (2013).
4. Gilkes, N. R., Kilburn, D. G., Miller, R. C. & Warren, R. A. Bacterial cellulases. *Bioresource Technology* **36,** 21–35 (1991).
5. Meyer, J. M. & Abdallah, M. A. The fluorescent pigment of Pseudomonas fluorescens: Biosynthesis, purification and physicochemical properties. *Journal of General Microbiology* **107** (1978).
6. Neilands, J. B. Iron absorption and transport in microorganisms. *Annual review of nutrition* **1** (1981).
7. Ringel, M. T. & Brüser, T. The biosynthesis of pyoverdines. *Microbial cell* **5,** 424–437 (2018).
8. Albrecht-Gary, A. M., Blanc, S., Rochel, N., Ocaktan, A. Z. & Abdallah, M. A. Bacterial iron transport: coordination properties of pyoverdin PaA, a peptidic siderophore of Pseudomonas aeruginosa. *Inorganic Chemistry* **33** (1994).
9. Bonneau, A., Roche, B. & Schalk, I. J. Iron acquisition in Pseudomonas aeruginosa by the siderophore pyoverdine: an intricate interacting network including periplasmic and membrane proteins. *Scientific Reports* **10,** 120 (2020).
10. West, S. A., Diggle, S. P., Buckling, A., Gardner, A. & Griffin, A. S. The social lives of microbes. *Annual Review of Ecology, Evolution, and Systematics* **38,** 53–77 (2007).
11. Buckling, A. *et al.* Siderophore-mediated cooperation and virulence in Pseudomonas aeruginosa. *FEMS Microbiology Ecology* **62,** 135–141 (2007).
12. Rainey, P. B., Desprat, N., Driscoll, W. W. & Zhang, X.-X. Microbes are not bound by sociobiology: Response to Kümmerli and Ross-Gillespie (2013). *Evolution* **68,** 3344–3355 (2014).
13. Zhang, X.-X. & Rainey, P. B. Exploring the sociobiology of pyoverdin-producing Pseudomonas. *Evolution* **67,** 3161–3174 (2013).

14. Julou, T. *et al.* Cell-cell contacts confine public goods diffusion inside Pseudomonas aeruginosa clonal microcolonies. *Proceedings of the National Academy of Sciences of the United States of America* **110,** 12577–82 (2013).

15. Jin, Z. *et al.* Conditional privatization of a public siderophore enables Pseudomonas aeruginosa to resist cheater invasion. *Nature Communications* **9,** 1383 (2018).

16. Hansen, S. K., Rainey, P. B., Haagensen, J. A. & Molin, S. Evolution of species interactions in a biofilm community. *Nature* **445** (2007).

17. Cordero, O. X. & Datta, M. S. Microbial interactions and community assembly at microscales. *Current Opinion in Microbiology,* 227–234 (2016).

18. Co, A. D., van Vliet, S., Kiviet, D. J., Schlegel, S. & Ackermann, M. Short-range interactions govern the dynamics and functions of microbial communities. *Nature Ecology and Evolution* **4,** 366–375 (2020).

19. Hartmann, R. *et al.* Emergence of three-dimensional order and structure in growing biofilms. *Nature Physics* **15,** 251–256 (2019).

20. Silby, M. W. *et al.* Genomic and genetic analyses of diversity and plant interactions of Pseudomonas fluorescens. *Genome Biology* **10,** R51 (2009).

21. Moon, C. D. *et al.* Genomic, genetic and structural analysis of pyoverdine-mediated iron acquisition in the plant growth-promoting bacterium Pseudomonas fluorescens SBW25. *BMC Microbiology* **8,** 7 (2008).

22. Hammerschmidt, K., Rose, C. J., Kerr, B. & Rainey, P. B. Life cycles, fitness decoupling and the evolution of multicellularity. *Nature* **515,** 75–9 (2014).

23. Spiers, A. J., Kahn, S. G., Bohannon, J., Travisano, M. & Rainey, P. B. Adaptive divergence in experimental populations of Pseudomonas fluorescens. I. Genetic and phenotypic bases of wrinkly spreader fitness. *Genetics,* 33–46 (2002).

24. Özkaya, Ö., Balbontín, R., Gordo, I. & Xavier, K. B. Cheating on cheaters stabilizes cooperation in Pseudomonas aeruginosa. *Current Biology* **28,** 2070–2080.e6 (2018).

25. Yeterian, E. *et al.* Synthesis of the siderophore pyoverdine in Pseudomonas aeruginosa involves a periplasmic maturation. *Amino Acids* **38,** 1447–1459 (2010).

26. Yeterian, E., Martin, L. W., Lamont, I. L. & Schalk, I. J. An efflux pump is required for siderophore recycling by Pseudomonas aeruginosa. *Environmental Microbiology Reports* **2,** 412–418 (2009).

27. Schalk, I. J. *et al.* Iron-free pyoverdin binds to its outer membrane receptor FpvA in Pseudomonas aeruginosa: a new mechanism for membrane iron transport. *Molecular Microbiology* **39,** 351–361 (2001).

28. Schalk, I. J. & Guillon, L. Pyoverdine biosynthesis and secretion in Pseudomonas aeruginosa : implications for metal homeostasis. *Environmental Microbiology* **15,** 1661–1673 (2013).

29. McDonald, M. J., Gehrig, S. M., Meintjes, P. L., Zhang, X.-X. & Rainey, P. B. Adaptive divergence in experimental populations of Pseudomonas fluorescens. IV. Genetic constraints guide evolutionary trajectories in a parallel adaptive radiation. *Genetics* **183,** 1041–53 (2009).

30. Quistad, S. D., Doulcier, G. & Rainey, P. B. Experimental manipulation of selfish genetic elements links genes to microbial community function. *Philosophical Transactions of the Royal Society B: Biological Sciences* **375,** 20190681 (2020).

31. Zhang, X.-X. *et al.* Genotypic and phenotypic analyses reveal distinct population structures and ecotypes for sugar beet-associated Pseudomonas in Oxford and Auckland. *Ecology and Evolution* **10,** 5963–5975 (2020).

32. Cornelis, P. & Matthijs, S. Diversity of siderophore-mediated iron uptake systems in fluorescent pseudomonads: Not only pyoverdines. *Environmental Microbiology* **4,** 787–798 (2002).

33. Shapiro, L., McAdams, H. H. & Losick, R. Generating and exploiting polarity in bacteria. *Science* **298,** 1942–1946 (2002).

34. Laloux, G. & Jacobs-Wagner, C. How do bacteria localize proteins to the cell pole? *Journal of Cell Science* **127** (2013).

35. Guillon, L., El Mecherki, M., Altenburger, S., Graumann, P. L. & Schalk, I. J. High cellular organization of pyoverdine biosynthesis in Pseudomonas aeruginosa: clustering of PvdA at the old cell pole. *Environmental Microbiology* **14,** 1982–1994 (2012).

36. Gasser, V., Guillon, L., Cunrath, O. & Schalk, I. Cellular organization of siderophore biosynthesis in Pseudomonas aeruginosa: Evidence for siderosomes. *Journal of Inorganic Biochemistry* **148,** 27–34 (2015).

37. Shi, H. *et al.* Starvation induces shrinkage of the bacterial cytoplasm. *Proceedings of the National Academy of Sciences* **118,** e2104686118 (2021).

38. Remigi, P. *et al.* Ribosome provisioning activates a bistable switch coupled to fast exit from stationary phase. *Molecular Biology and Evolution* **36,** 1056–1070 (2019).

39. Gore, J., Youk, H. & van Oudenaarden, A. Snowdrift game dynamics and facultative cheating in yeast. *Nature* **459,** 253–6 (2009).

40. Scholz, R. L. & Greenberg, E. P. Sociality in Escherichia coli: Enterochelin is a private good at low cell density and can be shared at high cell density. *Journal of Bacteriology* **197,** 2122–2128 (2015).

41. Tarnita, C. E. The ecology and evolution of social behavior in microbes. *Journal of Experimental Biology* **220** (2017).

42. Smith, E. E., Sims, E. H., Spencer, D. H., Kaul, R. & Olson, M. V. Evidence for diversifying selection at the pyoverdine locus of Pseudomonas aeruginosa. *Journal of Bacteriology* **187,** 2138–2147 (2005).

43. Bodilis, J. *et al.* Distribution and evolution of ferripyoverdine receptors in Pseudomonas aeruginosa. *Environmental Microbiology* **11,** 2123–2135 (2009).

499 44. Minandri, F. *et al.* Role of iron uptake systems in pseudomonas aeruginosa virulence and airway
500 infection. *Infection and Immunity* **84,** 2324–2335 (2016).

501 45. Taguchi, F. *et al.* The siderophore pyoverdine of Pseudomonas syringae pv. tabaci 6605 is
502 an intrinsic virulence factor in host tobacco infection. *Journal of Bacteriology* **192,** 117–126
503 (2010).

504 46. Trapet, P. *et al.* The Pseudomonas fluorescens siderophore pyoverdine weakens Arabidopsis
505 thaliana defense in favor of growth in iron-deficient conditions. *Plant physiology* **171,** 675–93
506 (2016).

507 47. Kloepper, J. W., Leongt, J., Teintzet, M. & Schroth, M. N. Enhanced plant growth by
508 siderophores produced by plant growth-promoting rhizobacteria. *Nature* **286,** 885–886 (1980).

509 48. Haas, D. & Défago, G. Biological control of soil-borne pathogens by fluorescent pseudomonads.
510 *Nature Reviews Microbiology* **3,** 307–319 (2005).

511 49. Stilwell, P., Lowe, C. & Buckling, A. The effect of cheats on siderophore diversity in Pseu-
512 domonas aeruginosa. *Journal of Evolutionary Biology* **31,** 1330–1339 (2018).

513 50. Mirleau, P. *et al.* Fitness in soil and rhizosphere of Pseudomonas fluorescens C7R12 compared
514 with a C7R12 mutant affected in pyoverdine synthesis and uptake. *FEMS Microbiology Ecology*
515 **34,** 35–44 (2000).

516 51. Banin, E., Vasil, M. L. & Greenberg, E. P. Iron and Pseudomonas aeruginosa biofilm formation.
517 *Proceedings of the National Academy of Sciences* **102,** 11076–11081 (2005).

518 52. Sass, G. *et al.* Studies of Pseudomonas aeruginosa mutants indicate pyoverdine as the central
519 factor in inhibition of Aspergillus fumigatus biofilm. *Journal of Bacteriology* **200** (2018).

520 53. Sexton, D. J. & Schuster, M. Nutrient limitation determines the fitness of cheaters in bacterial
521 siderophore cooperation. *Nature Communications* **8,** 230 (2017).

522 54. Butaitė, E., Kramer, J., Wyder, S. & Kümmerli, R. Environmental determinants of pyoverdine
523 production, exploitation and competition in natural Pseudomonas communities. *Environmental*
524 *Microbiology* **20,** 3629–3642 (2018).

525 55. Zhang, X.-X. & Rainey, P. B. Genetic analysis of the histidine utilization (hut) genes in Pseu-
526 domonas fluorescens SBW25. *Genetics* **176,** 2165–76 (2007).

527 56. Zhang, X.-X. & Rainey, P. B. Construction and validation of a neutrally-marked strain of
528 Pseudomonas fluorescens SBW25. *Journal of Microbiological Methods* **71,** 78–81 (2007).

529 57. Stylianidou, S., Brennan, C., Nissen, S. B., Kuwada, N. J. & Wiggins, P. A. SuperSegger: robust
530 image segmentation, analysis and lineage tracking of bacterial cells. *Molecular Microbiology*
531 **102,** 690–700 (2016).

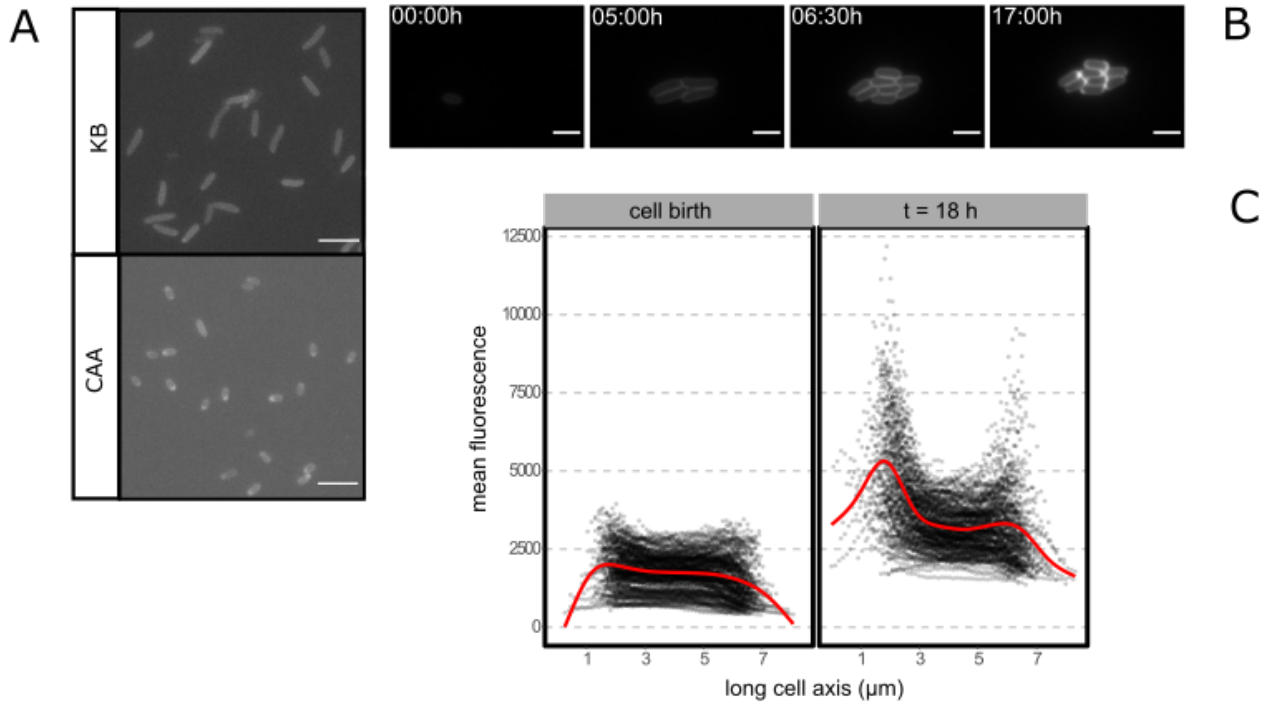

Figure 1: **Localization of pyoverdin in *P. fluorescens* SBW25 at the cell pole**. A) Snapshots of experiments described in [13] where fitness assays of pyoverdin producing SBW25 and a nonproducing *pvdS* defective mutant yield contrasting results depending on the culture medium. In both cases the environment is unstructured and ancestral SBW25 producer cells are rare, inoculated at 1%. A fitness advantage to nonproducing cells in KB was previously reported, but the reverse in CAA [13]. In KB (top) pyoverdin nonproducing cells rarely showed evidence of polar accumulation of pyoverdin, whereas (bottom) this was common in CAA cultured cells. Images were obtained from 3 μl samples of these experiments imaged under fluorescence light to visualize the distribution of pyoverdin. All scale bars correspond to 10 μm. B) Fluorescence time-lapse images of a growing microcolony of SBW25 in a SMM agarose pad. Images represent selected time points including, respectively: the initial inoculum, exponential growth, end of exponential growth (i.e. the final number of cells in the colony) and end of time-lapse acquisition (18 h total) C) Mean fluorescence intensity along the long axis of cells in a growing microcolony, when the last generation of cells is born (left) and at the end of acquistion (t = 18 h, right). Black dotted line represents the fluorescence profile of individual cells, the red line represents a smoothed mean of all the cells.

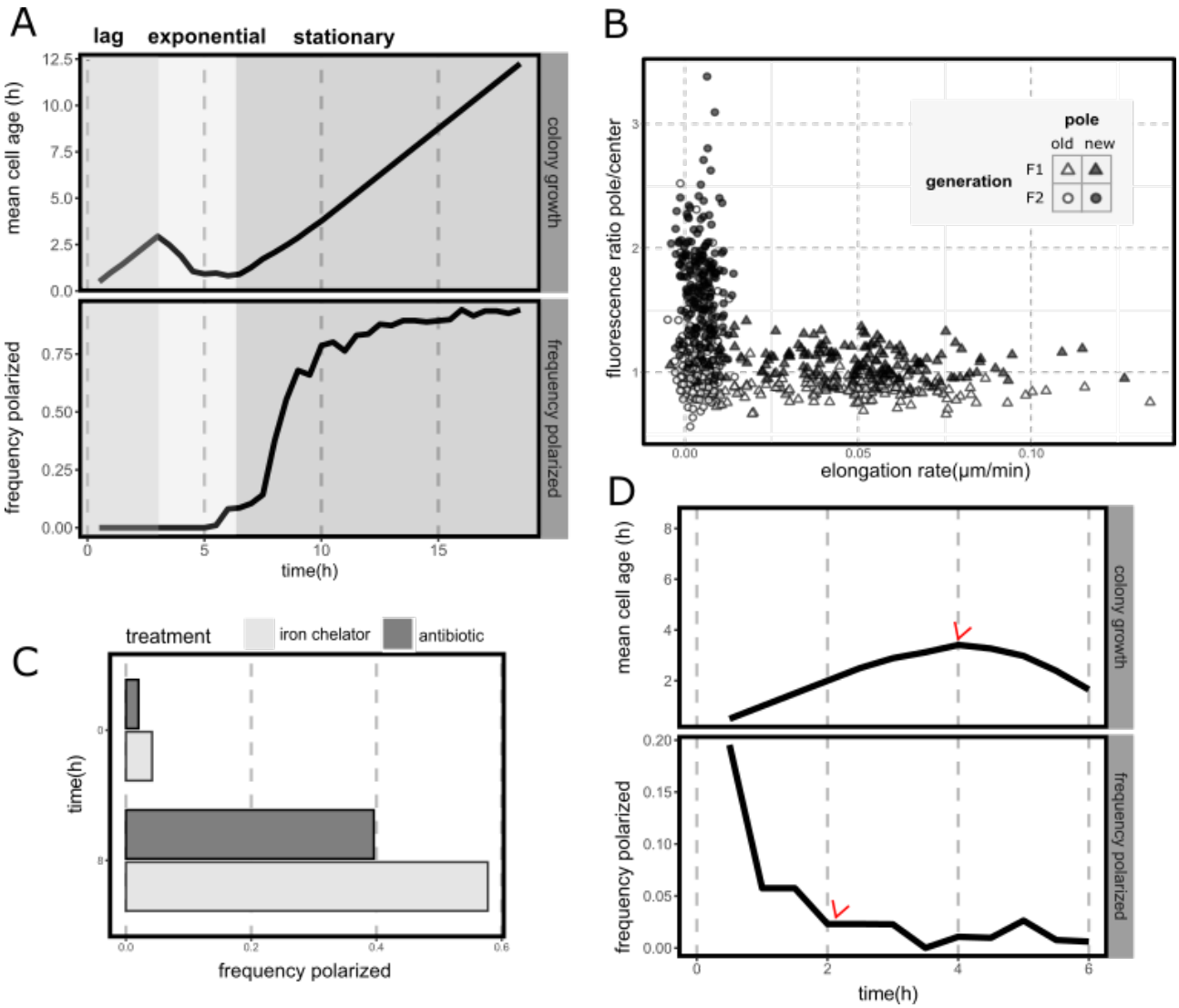

Figure 2: **Polarization is a reversible phenotype associated with arrest of cell division.** A) Polarization in different growth stages of a microcolony. Mean age of the cells in a growing microcolony of SBW25 (black line, top) and the corresponding frequency of polarized cells for each time point (black line, bottom). Colored panels represent the growth stages of the microcolony, from left to right: lag phase (generation F0), exponential phase (generation F1), and stationary phase (generation F2). N= 35, 159, 187 respectively. In all cases data has been filtered to exclude cells with segmentation errors or other artifacts that preclude proper analysis. Note that as microcolonies begin to form in exponential phase and cells are no longer isolated, overlap between adjacent cells creates regions of high fluorescence that could lead to classification errors. Nevertheless, visual inspection reveals that cells remain in a homogeneous state during exponential growth, with polarization onset being clearly associated to stationary phase. B) Elongation rate and accumulation of fluorescence at the cell pole of individual cells in a growing microcolony. Data extracted from A). Markers represent individual cells in different growth phases of the colony (F1, exponential, triangle markers; F2, stationary, circle markers) and the old (white markers) and new (black markers) cell pole. Elongation rate is represented by the average over the lifetime of a cell. Accumulation of fluorescence at the pole is represented by the maximum ratio over the lifetime of a cell of the sum of the pixels in the pole region and central region of a cell. These regions are defined by segmenting the cell and dividing it in 3 portions over the long axis, where the external $1/3$ represent each pole and the remaining $1/3$ represents the center. C) Polarization in response to chemical stresses related and unrelated to iron metabolism. Bars represent the frequency of polarized cells at the start of treatment and after 8h of treatment with either 100 μg/ml 2,2'-dipyridil (DP) (light bars) or 5 μg/ml tetracycline (dark bars). No cell division was observed during treatment. N = 99 (t=0h), 94 (t = 8h) and N = 94 (t = 0h), 79 (t = 8h) for DP and tetracyline treatments respectively. D) Depolarization and subsequent growth of cells pre-treated with an iron chelator. Plot represents colony growth and polarization as in A). Cells were treated with 100 μg/ml DP during 4h, washed and inoculated on a fresh SMM agarose pad. Data corresponds to five technical replicates i.e., five positions on the agarose pad. Red arrows indicate the time point where the colony overall starts growing (top) and where the majority of the cells are depolarized (bottom). Total initial number of cells N=87.

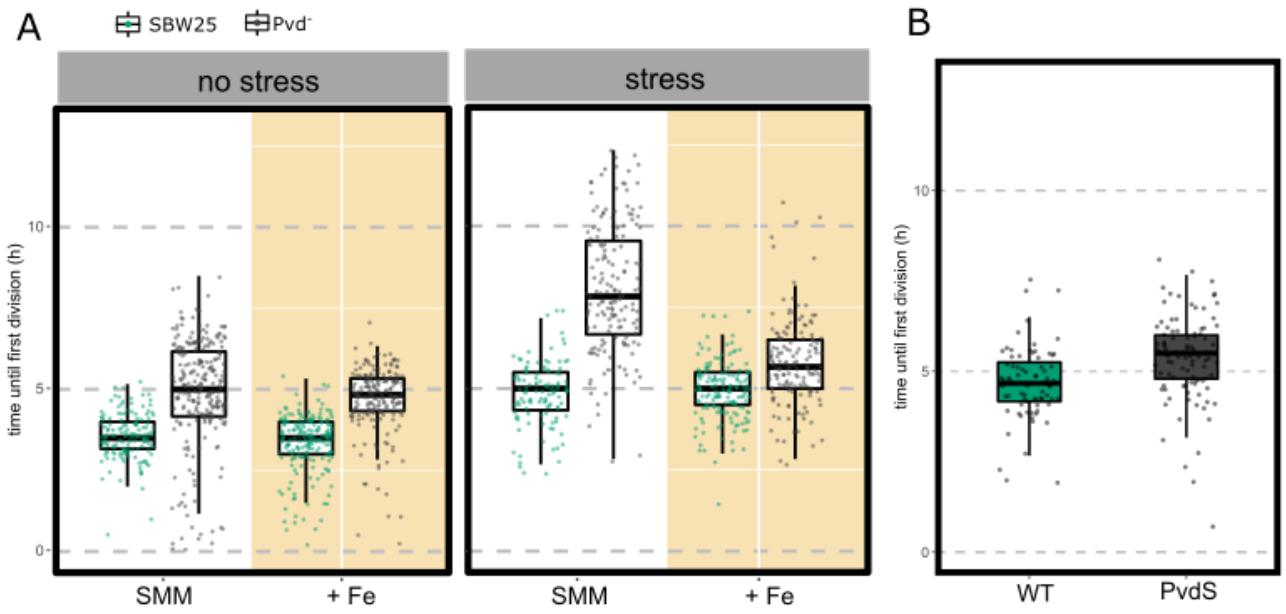

Figure 3: **Pyoverdin polarization facilitates recovery of growth after stress**.A) time until first division (lag time) of SBW25 (green) and pyoverdin defective mutant *pvdS229*(D77N), termed Pvd$^-$ (gray) under different treatments and conditions. Prior to inoculation cells were either grown in the usual culture medium SMM (no stress) or treated with DP for 4h (stress). This treatment was previously demonstrated to induce polarization while preventing cell division. Cells were then inoculated on a fresh agarose pad, supplemented with 0.45 mM $Fe_2[SO_4]_3$ where labeled "+ Fe" (yellow background) or in unmodified SMM medium (labeled "SMM", white background). Dots represent individual cell values, box plots represent the associated distribution (median, 25th and 75h percentiles) N = 145, 261, 199, 193, 111, 168, 156, 156 respectively from left to right. B) time until first division of SBW25 (green) and Pvd$^-$ mutants co-inoculated in a fresh agarose pad after separate stress treatment. Pvd$^-$ mutants were labeled with a red fluorescent protein to allow identification of individual cells on the pad. Dots and box plots as in A). N = 175 total cells.

A

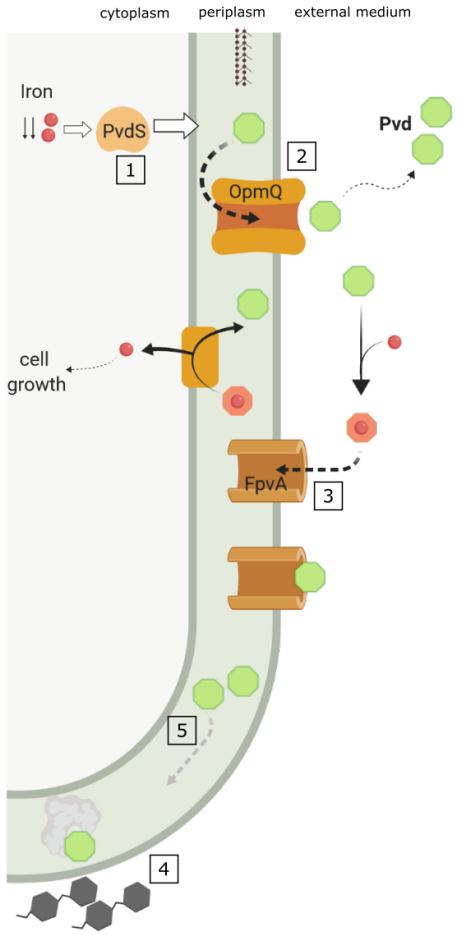

B

process	mutation	phenotype	conclusion
1 **synthesis**	*pvdSG229A*	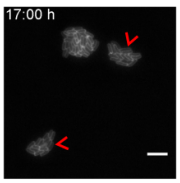	Cells polarize mature Pvd and import/ recycling machinery is sufficient.
2 **export**	*ΔopmQ*	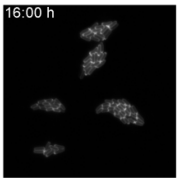	Pvd is not polarized bound to its main exporter.
3 **import**	*ΔfpvA*	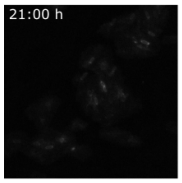	ΔFpvA mutants produce very small amounts of Pvd but some polarized cells can be found. Pvd is not polarized bound to its receptor.
4 **secreted polymers**	*Δwsp Δaws Δmws*	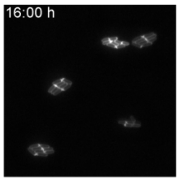	Pyoverdin is not polarized on the outside of the cells associated to polymers such as cellulose.
5 **cell shape**	*ΔmreB*	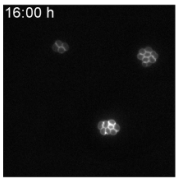	Polarization cannot be attributed to the rod shape morphology of *Pseudomonas.*

Figure 4: **Towards untangling the mechanism of polarization.** A) Cartoon depicting a simplified version of the pyoverdin pathway emphasizing potential mechanisms for pyoverdin polarization. 1. Pyoverdin (Pvd) synthesis starts in the periplasm in response to iron scarcity mediated by the transcription factor PvdS. Pyoverdin is then secreted to the bacterial periplasm, where it matures and becomes fluorescent. 2. Periplasmic pyoverdin is exported into the external medium by a complex that includes the transporter OpmQ. There, it chelates insoluble iron (Fe^{3+}). 3. Ferripyoverdin complexes (no longer fluorescent) are then imported back into the periplasm after binding to the receptor FpvA. This receptor is known to also bind free pyoverdin [7]. In the periplasm, iron is extracted and pyoverdin is again recycled into the external medium by OpmQ. Polarization might also be caused by mechanisms unrelated to the pyoverdin pathway: 4. SBW25 is known to secrete polymers such as cellulose where pyoverdin molecules could be trapped [23]. 5. Pyoverdin could accumulate at the cell poles due to the rod shape of SBW25. An alternative option is presented, where pyoverdin could bind another yet unidentified periplasmic protein (in gray). B) Mutants associated to the main processes depicted in A) and their phenotype with regards to pyoverdin polarization. Mutants were grown on an agarose pad as described and fluorescence images displaying pyoverdin were taken at the time points indicated in the photo. The pyoverdin nonproducing mutant *pvdSG229A*(D77N) was co-inoculated with SBW25 to enable access of the mutant to pyoverdin. Mutants were tagged with red a fluorescent protein, mutant colonies are labeled with a red arrow on the image.

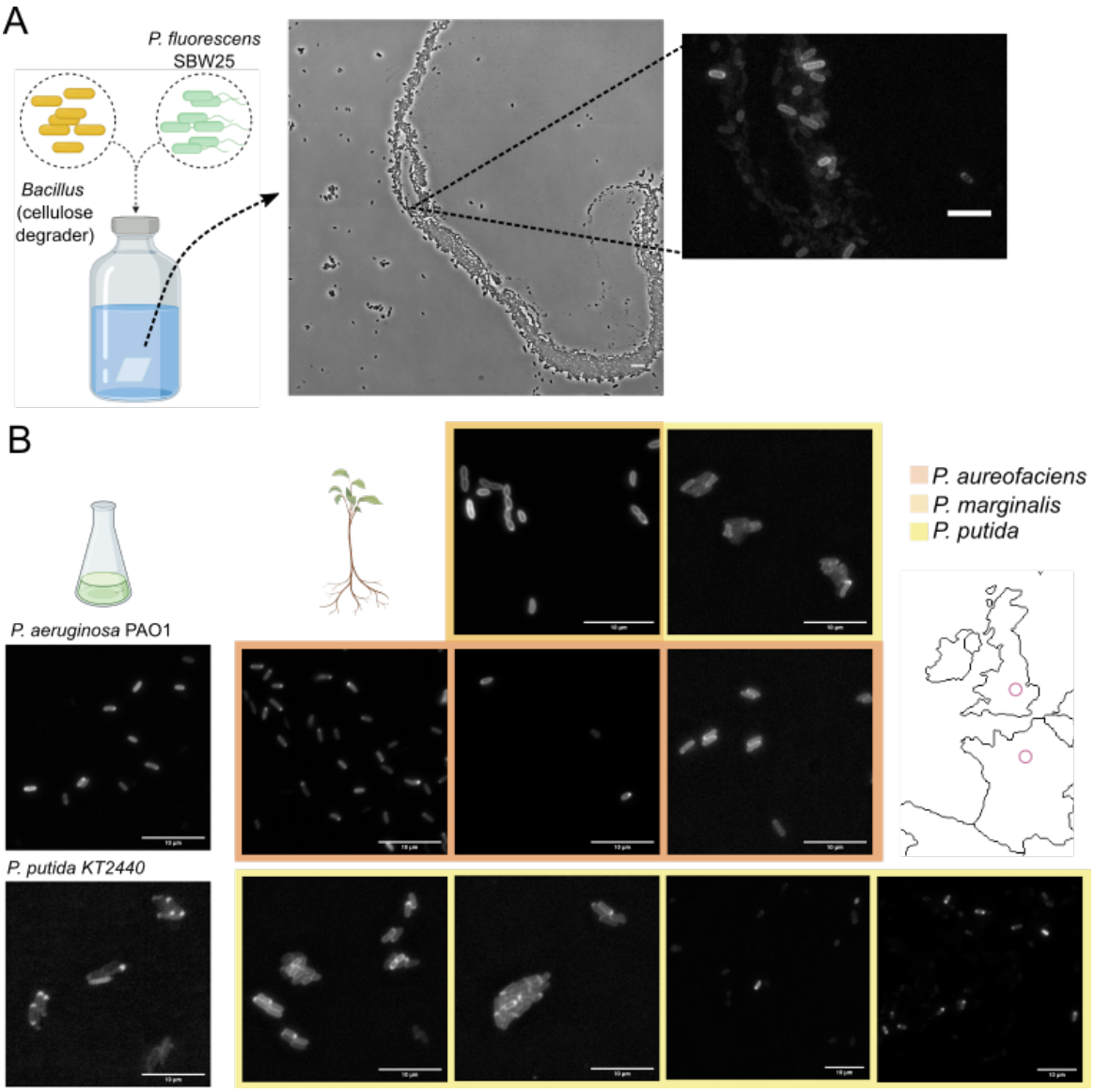

Figure 5: **Polarization is evident in SBW25 in a multispecies community and is a common phenotype in related species of the genus *Pseudomonas*** A) Polarized SBW25 cells in a multispecies community with interdependencies. SBW25 and a celluose-degrading *Bacillus* strain isolated from a compost heap in Paris, France [30] were co-cultured in glass vials with minimal medium and cellulose paper as the only carbon source. The community was periodically sampled to assess the polarization state of SBW25. A representative image obtained after 28 days of growth is displayed, where both strains are visible (left, phase contrast image) and in a magnified region where pyoverdin distribution in SBW25 is visualized (right, fluorescence image). B) Qualitative polarization assessment in species of *Pseudomonas* other than SBW25. A collection of laboratory (left) and natural (right) strains were tested for polarization in conditions equivalent to SBW25 and adapted to each isolate: SMM amended with the iron chelator DP where indicated, in liquid medium or on agarose pads as previously described, and observed by fluorescence microscopy. Natural isolates were collected in Oxford, UK [31] (first and second row) and in Paris, France [30] (Bottom row)(locations are roughly marked with a pink circle on the map). Color represents the identified *Pseudomonas* species. left) Polarization test in commonly used laboratory strains: *P. aeruginosa* PAO1 (tested in SMM agarose pad with 1000 μg/ml DP for 7:30 h), and *P. putida* KT2440 (SMM agarose pad, 24h). right) Polarization test in natural isolates, left to right and top to bottom: U106 (liquid KB medium, 24 h), U177 (SMM agarose pad, 24 h), U149 (liquid SMM with DP 100 μg/ml, 24 h), U180 (liquid SMM with DP 100 μg/ml, 24), U181 (SMM agarose pad, 16 h), T24 V1a (SMM agarose pad, 24 h), T24 V9b (SMM agarose pad, 24 h), T24 H1b (SMM agarose pad, 24 h), T24 H9b (liquid SMM, 24 h).